

Topological invariants based on generalized position operators and application to the interacting Rice-Mele model

A. A. Aligia¹

¹*Instituto de Nanociencia y Nanotecnología CNEA-CONICET,
Centro Atómico Bariloche and Instituto Balseiro, 8400 Bariloche, Argentina*

We discuss different properties and the potential of several topological invariants based on position operators to identify phase transitions, and compare with more accurate methods, like crossing of excited energy levels and jumps in Berry phases. The invariants have the form $\text{Im} \ln \langle \exp [i(2\pi/L)\Sigma_j x_j (m_\uparrow \hat{n}_{j\uparrow} + m_\downarrow \hat{n}_{j\downarrow})] \rangle$, where L is the length of the system, x_j the position of the site j , and $\hat{n}_{j\sigma}$ the operator of the number of particles at site j with spin σ . We show that m_σ should be integers, and in some cases of magnitude larger than 1 to lead to well defined expectation values. For the interacting Rice-Mele model (which contains the interacting Su-Schrieffer-Heeger and the ionic Hubbard model as specific cases), we show that three different invariants give complementary information and are necessary and sufficient to construct the phase diagrams in the regions where the invariants are protected by inversion symmetry. We also discuss the consequences for pumping of charge and spin, and the effect of an Ising spin-spin interaction or a staggered magnetic field.

I. INTRODUCTION

Many transitions in condensed matter has been understood as a spontaneous symmetry breaking and the emergence of a local order parameter as the temperature is lowered¹. However, there are other transitions, which are the subject of much attention recently, in which two different phases differ in the value of a symmetry protected topological invariant^{2–11}. While significant advances have been made at the single-particle level, more recent studies have addressed many-body cases^{7,11–16}.

A difference with the non-interacting case is that the presence of zero-energy edge modes dictated by the bulk-boundary correspondence, is modified by the possible presence of zeros of the interacting Green's functions at zero energy^{12,13}. Interestingly, these zeros are responsible for a topological transition in a two-channel spin-1 Kondo model with easy-plane anisotropy¹⁷.

Many of the topological invariants used are extensions of the Berry phase calculated by Zak for a one-particle state as the wave vector sweeps the entire Brillouin zone in one dimension¹⁸ (see for example Refs. 6, 16, 19–22). This *charge* Berry phase γ_c is in turn the basis of the modern theory of polarization^{23–26}, and has been extended to the many-body case^{27–30} and to multipoles^{31,32}. Changes in γ_c are proportional to changes in the polarization of the system²⁷. We have introduced the *spin* Berry phase γ_s , which is a measure of the difference of polarizations between electrons with spin up and down³³.

In systems with inversion symmetry, both phases are protected by this symmetry and can take only the values 0 or π . Thus, they are Z_2 topological invariants and have been used to identify quantum phase transitions^{27,34–37} and in particular to construct the phase diagram of the Hubbard chain with correlated (density-dependent) hopping (HCCH)³⁴ and the ionic Hubbard chain (the Hubbard model with alternating on-site energies discussed

in more detail in Section IV)³⁶. Furthermore for these two models, it has been shown³⁶ that the jumps of the Berry phases coincide with crossings of energy levels which are known to correspond to phase transitions determined by the method of crossing of excited energy levels (MCEL) based on conformal field theory^{38–42}. Therefore, the results extrapolated to the thermodynamic limit are expected to be highly accurate and more efficient than calculating correlation functions, which change in a smooth fashion at the transitions in finite systems. For the HCCH the phase diagram obtained from jumps in the Berry phases coincides with that obtained from bosonization^{43,44} for small values of the interaction.

Using results of the MCEL³⁹, it has been shown that for systems with spin SU(2) symmetry, the jump of the spin Berry phase indicates the opening of a spin gap³³. In a Kosterlitz-Thouless transition, the spin gap opens exponentially at it is very difficult to identify the transition point from a direct calculation of the spin gap in large systems. It is much more efficient to determine these point extrapolating the jumps in the topological invariant for small systems³⁴.

Resta^{45,46} has shown (for an integer number of particles per unit cell) that in the thermodynamic limit, the polarization and the charge Berry phase, can be calculated from a ground state expectation value as $\alpha(1,1)$ with

$$\alpha(m_\uparrow, m_\downarrow) = \text{Im} \ln \langle U(m_\uparrow, m_\downarrow) \rangle \mod 2\pi, \quad (1)$$

where

$$U(m_\uparrow, m_\downarrow) = \exp [i(2\pi/L)\Sigma_j x_j (m_\uparrow \hat{n}_{j\uparrow} + m_\downarrow \hat{n}_{j\downarrow})], \quad (2)$$

L is the length of the system, x_j the position of the site j , $\hat{n}_{j\sigma}$ the operator of the number of particles at site j , and m_σ are integers. Although this expectation value is expected to be less accurate than the charge Berry phase for a finite system, it is easier to calculate, and has been

used extensively. For a non-interacting system, Resta has shown that $\alpha(1, 1)$ coincides with the charge Berry phase in the thermodynamic limit⁴⁵. One expects that this is also true in the interacting case. This is supported by our calculations in a specific interacting model presented in Section VI A.

Soon it was noticed that in turn, at zero temperature, $\alpha(1, -1)$ is an approximation to the spin Berry phase γ_s ³⁴, which is expected to coincide with it (except for a sign, as explained in Section III) in the thermodynamic limit.

If the total number of particles per unit cell N/N_{uc} is an irreducible fraction p/l , $\alpha(1, 1)$ is ill defined and should be replaced by $\alpha(l, l)$ ⁴⁷. In general, the conditions that m_σ should fulfill to lead to well defined $\alpha(m_\uparrow, m_\downarrow)$ are discussed in Section III. The quantity

$$x(l, l) = \frac{a}{2\pi l} \alpha(l, l) \bmod \frac{a}{l}, \quad (3)$$

where a is the lattice parameter, is a well defined expectation value of the sum of the positions of the particles per unit cell^{47,48}. Recently it has been shown that $\alpha(l, l)$ is a topological invariant at finite temperature¹⁴. At zero temperature, the quantity $\alpha(l, -l)$ pointed out in Ref. 34 as an alternative to calculate the spin the Berry phase for $l = 1$, was used by Nakamura and Todo to study resonance-valence-bond states in spin systems⁴⁹, using the symmetry properties explained in Ref. 47. The operator of Eq. (2) has also being generalized as a tensor for different spin and position directions, allowing to express the ferrotoroidic moment as a quantum geometric phase⁵⁰. Cumulants of $\alpha(l, l)$ ^{51,52} were also used to identify phase transitions⁵³⁻⁵⁵, and $\langle U(1, 1) \rangle$ was used to study scaling in disordered systems⁵⁶.

A Thouless pump can be regarded as a cycle in a space of parameters in which a quantized amount of charge (or spin) is transported, which is topologically protected^{57,58}. Experimentally quantized charge pumping has been realized in ultracold quantum-gas experiments that simulate the fermionic⁵⁹ and bosonic⁶⁰ Rice-Mele model (RMM)⁶¹. A spin pump was also realized experimentally⁶². Recently charge pumping in the fermionic interacting RMM (IRMM) has been studied experimentally⁶³ and theoretically⁶⁴⁻⁶⁶. For a recent review of Thouless pumping and topology, see Ref. 67.

The RMM contains the Su-Schrieffer-Heeger model (SSH)⁶⁸ as a special case, with alternating hopping matrix elements $t \pm \delta$. For the spinless SSH or the non-interacting case choosing one spin, two different topological states exists depending on the sign of δ , which are characterized by different Zak Berry phases, either 0 or $\pi \bmod 2\pi$ ²⁰. While the charge and spin transport in the adiabatic limit of the IRMM can be well described in terms of the charge and spin Berry phases described above, or equivalently by $\alpha(1, 1)$ and $\alpha(1, -1)$ ⁶⁶, these quantities are unable to separate the two topological phases of the SSHM. This is expected, because since the average position (or polarization) of the particles for

both spins is the same, and 0 or $\pi \bmod 2\pi$, adding or subtracting them gives 0 $\bmod 2\pi$ in both cases. Recently, a study of the SSHM at finite temperatures found $\alpha(1, 0) = \pm\pi/2$ in some cases⁶⁹. In addition, in a recent study on the strongly-interacting SU(3) SSHM, it has been stated that a Berry phase in which the flux is applied only to one of the flavors [related to $\alpha(1, 0)$ or $\alpha(0, 1)$ in the SU(2) case] can distinguish between the two topological sectors.

In this paper we discuss for the general case, the conditions on the m_σ so that the generalized position operators are well defined. They should be integers and it is convenient to choose them as the smallest possible integers that guarantee translationally invariant position operators. We also study their properties under inversion and their relation with the Berry phases. The discussion is restricted to one dimension and two flavors, but it can be generalized. For the specific IRMM, and parameters for which the system has inversion symmetry, we compare the topological transitions predicted from jumps in several $\alpha(m_\uparrow, m_\downarrow)$ with alternative methods. The size dependence of the transitions is also studied. We find that to obtain a complete picture of the topological sectors, three different invariants should be considered, $\alpha(1, 1)$, $\alpha(1, -1)$ and either $\alpha(1, 0)$ or $\alpha(0, 1)$. We also discuss the effect of terms that open the spin gap, like an Ising interaction and staggered magnetic field⁶⁶. Finally we used the generalized position operators to analyze the charge and spin transport in pump cycles.

The paper is organized as follows. In Section II we briefly review the calculation of the Berry phases and its relation to the modern theory of polarization in the many-body case. This facilitates the explanation of the position expectation values and its symmetry properties for general Hamiltonians discussed in Section III. In Section IV we explain the IRMM with possible addition of Ising spin-spin interactions and staggered magnetic field, which is used for numerical calculations in Section VI. In Section V we discuss the form of some general symmetry properties discussed in Section III to particular cases of the IRMM. In Section VI we present different calculations using exact diagonalization, in systems up to 14 sites, to compare the predictions of the phase transitions obtained from jumps in the topological invariants based on position operators, with other (in general more robust) known results. We also study some pump cycles which shed light on the potential and limitations of the different position operators. Section VII contains a summary and discussion.

II. BERRY PHASES AND MANY-BODY POLARIZATION

For the discussion of the topological invariants, it is useful to briefly review the formulation of the Berry phases and the modern theory of polarization for many-body systems. This theory is basically an extension

of the formalism of Zak for non-interacting particles¹⁸. Restricting to one-dimension, Zak calculated the Berry phase of a Bloch state as the wave vector k sweeps all possible values $0 \leq k \leq 2\pi/a$, where a is the lattice parameter. This is equivalent to consider all possible twisted boundary conditions defined by a flux Φ through a ring. To simplify the argument, ignore spin for the moment and consider that the hopping term of the Hamiltonian has the form (extension to more involved cases are straightforward)

$$H_t = -t \sum_{j=1}^{N_s-1} c_{j+1}^\dagger c_j - t e^{i\Phi} c_1^\dagger c_{N_s} + \text{H.c.}, \quad (4)$$

where N_s is the number of sites. The Hamiltonian can be interpreted as a periodic chain with boundary conditions such that a translation of a one-particle state T_L in the size of the system $L = aN_{uc}$, where N_{uc} is the number of unit cells, gives

$$T_L c_j^\dagger |0\rangle = e^{i\Phi} c_j^\dagger |0\rangle. \quad (5)$$

The eigenstates of the translation operator with a given wave vector k satisfy

$$T_a c_k^\dagger |0\rangle = e^{ika} c_k^\dagger |0\rangle. \quad (6)$$

Eqs. (5), (6) and $T_a^{N_{uc}} = T_L$ imply that the possible values of k are

$$ka = \frac{2\pi\nu + \Phi}{N_{uc}}. \quad (7)$$

with ν integer. Then, changing adiabatically the flux is equivalent to changing the one-particle wave vectors.

For a periodic many-body system with conserved number of particles N , the total wave vector K is conserved, and the change in K under an adiabatic change in Φ is given by

$$\Delta K a = \frac{N}{N_{uc}} \Delta \Phi. \quad (8)$$

Then, if the number of particles per unit cell N/N_{uc} is an integer, and if a given state (in particular the ground state) is non degenerate as Φ is swept from 0 to 2π , the ground state returns to the ground state and captures a Berry phase. If however, N/N_{uc} is fractional, the state at $\Phi = 2\pi$ is different from that at $\Phi = 0$ (it has a different total wave vector) and the cycle should be extended to the region $0 \leq \Phi \leq 2\pi l$, with lN/N_{uc} integer^{33,47}

In practice, it is convenient to perform a gauge transformation

$$c_j^\dagger = \exp(i\Phi x_j/L) \tilde{c}_j^\dagger, \quad (9)$$

where x_j is the position of the site j , so that the hopping term becomes explicitly translationally invariant

$$H_t = -t \exp(i\Phi b/L) \left(\sum_{j=1}^{N_{uc}-1} \tilde{c}_{j+1}^\dagger \tilde{c}_j + \tilde{c}_1^\dagger \tilde{c}_{N_s} \right) + \text{H.c.}, \quad (10)$$

where b is the nearest-neighbor distance. In the more general cases studied below, we take also a translationally invariant form of the Hamiltonian.

The Berry phases considered here can be calculated from the numerically gauge invariant formulation^{27,33}, splitting the interval of the flux $0 \leq \Phi \leq 2\pi l$ in M parts.

$$\gamma(m_\uparrow, m_\downarrow) = -\lim_{M \rightarrow \infty} \text{Im} \ln \left\{ \left[\prod_{r=0}^{M-2} \langle g(\Phi_r) | g(\Phi_{r+1}) \rangle \right] \times \langle g(\Phi_{M-1}) | U(m_\uparrow, m_\downarrow) g(0) \rangle \right\}, \quad (11)$$

where $|g(\Phi)\rangle$ is the ground state of the Hamiltonian in which the hopping from site i to site j for spin σ has been changed by a factor $\exp[im_\sigma(x_j - x_i)\Phi/L]$ and $U(m_\uparrow, m_\downarrow)$, given by Eq. (2) transforms the ground state for $\Phi = 0$ to that for $\Phi = 2\pi l$ using the gauge transformation Eq. (9). Usually the origin of coordinates x_j is chosen at an atomic position. If not, the Berry phase is modified by a constant as explained in Section III. In practice, a number of splittings $M \sim 10$ is enough to obtain accurate results.

The cases related with total charge $\gamma_c = \gamma(l, l)$ ^{27,33} and total spin $\gamma_s = \gamma(l', -l')$ ³³ have been studied before. From the modern theory of polarization in the many-body case, one knows that if the parameters of the Hamiltonian are changed as a function of a parameter θ , between θ_1 and θ_2 , the change of polarization (equivalent to the displacement of charge in one dimension), can be expressed in terms in the Berry phase γ_c . If the particles are electrons, the transported charge in units of e where $-e$ is the electronic charge, the transported charge is given by

$$\Delta Q = \frac{1}{2\pi l} \int_{\theta_1}^{\theta_2} d\theta \partial_\theta \gamma_c(\theta). \quad (12)$$

Similarly for the transported z projection $Q_s = Q_\uparrow - Q_\downarrow$ of the spin one has³³

$$\Delta Q_s = \frac{1}{2\pi l'} \int_{\theta_1}^{\theta_2} d\theta \partial_\theta \gamma_s(\theta). \quad (13)$$

One is tempting to suggest that similar expressions could be used for Q_σ in terms of $\gamma(1, 0)$ and $\gamma(0, 1)$ respectively. This is true in some cases, but not always. We return to this point later for the specific case of the IRMM.

In systems with inversion symmetry, and choosig the origin of coordinates at the inversion point, the result for the Berry phases should be the same if the sign of the flux Φ is inverted, which in turn leads to same Berry phase with the sign inverted implying $\gamma = -\gamma \bmod 2\pi$ ¹⁸.

Thus, in systems with inversion symmetry, γ/π is a topological Z_2 number protected by symmetry that can take only two values, 0 or 1 mod 2. This fact has been used to construct the complete phase diagram of the Hubbard model with density-dependent hopping³⁴ and the ionic Hubbard model³⁶ from the values of γ_c and γ_s or crossing of excited energy levels^{38–41} which coincide with jumps in these Berry phases for these models³⁶. In presence of a rotation symmetry of the spin in π around any axis perpendicular to the z axis [in particular in the presence of spin SU(2) symmetry], γ_s is also a Z_2 topological number protected by that symmetry⁶⁶.

III. GENERALIZED POSITION EXPECTATION VALUES

Generalizing previous developments, one can define position expectation values from Eqs. (1) and (2). In addition to the total position Eq. (3), one can define the expectation value of the sum of the positions of the electrons with spin up per unit cell as

$$x(m_\uparrow, 0) = \frac{a}{2\pi m_\uparrow} \alpha(m_\uparrow, 0) \bmod \frac{a}{m_\uparrow}, \quad (14)$$

where a is the lattice parameter, and similarly for spin down. For $S_z = 0$, the difference between the positions of the electrons with spin up and down per unit cell is

$$x(1, -1) = \frac{a}{2\pi} \alpha(1, -1) \bmod a. \quad (15)$$

In this Section we discuss the general properties of this quantities as well as some conditions imposed by symmetry.

Comparing Eqs. (1), (2) and (11) one realizes that except for the sign, the second member of Eq. (1) is a crude approximation to $\gamma(m_\uparrow, m_\downarrow)$, with only $M = 1$ point in the whole interval of flux $0 \leq \Phi \leq 2\pi l$. However, both quantities are expected to coincide in the thermodynamic limit⁴⁵, $\alpha(m_\uparrow, m_\downarrow)$ has the advantage over the Berry phases of its simplicity, its extension to finite temperature and the possibility to calculate it for open boundary conditions⁷⁰, which allows for more accurate density-matrix renormalization-group calculations. In addition, we find that in certain cases it is difficult to calculate $\gamma_s = \gamma(1, -1)$ directly because of level crossings that take place at finite values of the flux Φ .

In a ring, the positions of the particles x_j are defined modulo L . This means that that $x_j + L \equiv x_j$ should be satisfied. Thus for $x(m_\uparrow, m_\downarrow)$ to be well defined, the result should be invariant if for any j , x_j is replaced by $x_j + L$. Since the eigenvalues of $\hat{n}_{j\sigma}$ are either 0 or 1, the change in the exponent of Eq. (2) is a multiple of $2\pi i$ (irrelevant) for any states if and only if the m_σ are integers.

Under an elemental translation in a unit cell a one has

$$\begin{aligned} T_a U(m_\uparrow, m_\downarrow) T_a^\dagger &= \exp \left[i \frac{2\pi}{L} \sum_j (x_j + a)(m_\uparrow \hat{n}_{j\uparrow} + m_\downarrow \hat{n}_{j\downarrow}) \right] \\ &= \exp \left[i \frac{2\pi a}{L} (m_\uparrow \hat{N}_\uparrow + m_\downarrow \hat{N}_\downarrow) \right] U, \end{aligned} \quad (16)$$

where $\hat{N}_\sigma = \sum_j \hat{n}_{j\sigma}$ is the operator of the total number of particles with spin σ . For the last equality we used that any two $\hat{n}_{j\sigma}$ commute.

To be well defined, $U(m_\uparrow, m_\downarrow)$ should not depend of the unit cell in which the origin of x_j is chosen. Thus, the exponential should be equivalent to 1, and this imposes

$$\frac{a(m_\uparrow \hat{N}_\uparrow + m_\downarrow \hat{N}_\downarrow)}{L} = I = \text{integer}. \quad (17)$$

The first member should be a conserved quantity of the Hamiltonian. Eq. (17) implies in particular that for $U(l, l)$ to be well defined, the total number of particles $\hat{N} = \hat{N}_\uparrow + \hat{N}_\downarrow$ should be conserved, and if the number of particles per unit cell aN/L is an irreducible fraction, l should be chosen as the denominator (as shown before with a slightly different argument⁴⁷). For $U(l, -l)$, the total spin projection $S_z = (\hat{N}_\uparrow - \hat{N}_\downarrow)/2$ should be conserved. In the simplest case $S_z = 0$, it is convenient to choose $l = 1$. Finally if $m_\sigma = l$ and $m_{-\sigma} = 0$, it is convenient to choose the minimum l that satisfies that laN_σ/L is an integer. In usual cases with $S_z = 0$, and one particle per unit cell or less, this l is two times larger than the corresponding one for $U(l, l)$.

The above mentioned conservation laws imply that for an extension to finite temperatures of $\alpha(l, l)$ ¹⁴, the canonical ensemble should be used. This fact seems to have been overseen in a recent work⁶⁹.

Note that Eq. (16) is also valid if the lattice parameter is replaced by any finite displacement d . Following the same procedure as above, it is easy to see that

$$x_j \longrightarrow x_j + d \implies \alpha(m_\uparrow, m_\downarrow) \longrightarrow \alpha(m_\uparrow, m_\downarrow) + \frac{d}{a} 2\pi I, \quad (18)$$

where I is the integer entering Eq. (17). While the symmetry properties defined below take a different form for different d , this constant shift is however not important, since only differences in polarization have a physical meaning [see Eqs. (12) and (13)] and the magnitude of the jumps of $\alpha(m_\uparrow, m_\downarrow)$ at phase transitions remain the same.

While the calculation of the Berry phases imply an average over all twisted boundary conditions (BC), the calculation of the displacement operators are usually performed either for closed shell BC (CSBC), which correspond to antiperiodic BC for N_s multiple of four and periodic BC for even N_s not multiple of four, or for open shell BC (OSBC) in which periodic and antiperiodic BC

are interchanged with respect to CSBC. The results for both cases are compared in Sections VIA and VIB.

If the Hamiltonian is invariant under inversion R through certain atoms and the coordinates are defined in such a way that $x_j = 0$ for one of these atoms j , then using translations [Eq. (16)], one can define R such that $Rx_j = -x_j$. Clearly

$$RU(m_\uparrow, m_\downarrow)R^\dagger = \overline{U(m_\uparrow, m_\downarrow)}, \quad (19)$$

where the bar over U means complex conjugation. Since all eigenstates should be either even or odd under R , the expectation value of $U(m_\uparrow, m_\downarrow)$ should be real and this implies that the second member of Eq. (1) is either 0 or π , implying that it is a Z_2 topological invariant protected by R .

If however the inversion symmetry \tilde{R} has the invariant point at x_b between two atoms, one can define $\tilde{R}x_j = 2x_b - x_j$, which is equivalent to a change of sign of x_j plus a translation giving

$$\begin{aligned} & \tilde{R}U(m_\uparrow, m_\downarrow)\tilde{R}^\dagger \\ &= \exp \left[i \frac{4\pi x_b}{L} (m_\uparrow \hat{N}_\uparrow + m_\downarrow \hat{N}_\downarrow) \right] \overline{U(m_\uparrow, m_\downarrow)}. \end{aligned} \quad (20)$$

Implications for the particular case of the IRMM are discussed in Section V.

Note that the arguments above about topological protection by inversion symmetry applied to zero temperature, assume a non-degenerate ground state and breaks down in the thermodynamic limit if there is a spontaneous symmetry breaking. We return to this point in Section VIC.

IV. MODEL

To test explicitly the properties of different generalized position operators and its accuracy as topological Z_2 invariants to determine phase transitions, we consider the interacting Rice-Mele model (IRMM). The Hamiltonian is

$$\begin{aligned} H = & \sum_{j=0}^{N_s-1} [-t + \delta (-1)^j] \sum_{\sigma=\uparrow, \downarrow} \left(c_{j\sigma}^\dagger c_{j+1\sigma} + \text{H.c.} \right) \\ & + \Delta \sum_{j=0}^{N_s-1} \sum_{\sigma=\uparrow, \downarrow} (-1)^j \hat{n}_{j\sigma} + U \sum_{j=0}^{N_s-1} \hat{n}_{j\uparrow} \hat{n}_{j\downarrow}. \end{aligned} \quad (21)$$

For some calculations, we will also add to the Hamiltonian either an Ising spin-spin coupling H_Z or a staggered magnetic field H_B ⁶⁶

$$H_Z = J_z \sum_{j=0}^{N_s-1} S_j^z S_{j+1}^z, \quad H_B = B \sum_{j=0}^{N_s-1} (-1)^j S_j^z. \quad (22)$$

For $\delta = 0$, the model reduces to the ionic Hubbard model (IHM)^{36,71,72}, which has inversion symmetry with center at any site, and for $\Delta = 0$, it coincides with the interacting SSHM (ISSHM) which has inversion symmetry with center at the midpoint between any two sites. In both cases, the Berry phases and the position operators become topological Z_2 invariants protected by the corresponding inversion symmetry. Our discussion here is limited to zero temperature, number of particles equal to the number of sites ($N = N_s$) and total spin $S_z = 0$. Then, there are two particles per unit cell ($N_{uc} = N_s/2$) and the smallest integers $l = 1, m_\sigma = 1$ are enough to have well defined Berry phases and position operators [see Eqs. (3) and (14)] (this is not the case for extensions of the model to more sites per unit cell⁷³).

Therefore, in the following we define $\alpha_c = \alpha(1, 1)$, $\alpha_s = \alpha(1, -1)$, $\alpha_\uparrow = \alpha(1, 0)$, and $\alpha_\downarrow = \alpha(0, 1)$, for the charge, spin and spin σ only expectation values. We take the position of lattice site 0 as the origin ($x_0 = 0$) [if the origin were taken between two lattice sites, so that $x_0 = a/4$, α_c would be shifted by π , α_σ by $\pi/2$ and α_s would remain the same according to Eq. (18)].

The phase diagram of the IHM has been determined accurately using topological Z_2 invariants³⁶. A numerical study of different correlation functions has been performed by Manmana *et al.*⁷². The half-filled IHM hosts three phases. For $t \rightarrow 0$, there are only two phases, a band insulating (BI) phase with alternating occupancies 0202... or 2020... depending on the sign of Δ for $U < 2|\Delta|$ and a Mott insulating phase with one-particle per site, described by an effective Heisenberg model⁷⁴ for $U > 2|\Delta|$. At finite t , a spontaneously dimerized insulator (SDI) with a bond-ordering wave (BOW)⁷¹ appears between the other two phases and the boundaries move to larger U ³⁶. At the BI to SDI transition, the charge Berry phase γ_c jumps from 0 to π , while at the SDI to MI transition, the spin Berry phase γ_s jumps from 0 to π .

The BOW corresponds to stronger expectation values of the hopping for odd than even bonds or conversely [see Eq. (27)]. The SDI corresponds to one of these choices in the thermodynamic limit. A finite δ breaks the inversion symmetry and renders one of the BOW phases more favorable than the other, and also the MI phase is converted to a BOW phase⁶⁶.

The SSHM has two phases that can be distinguished by the Berry phase for one spin²⁰. In the ISSHM ($U > 0$), the same behavior is expected¹⁶, although the zero-energy one-particle modes related to the topological phase disappear¹³.

V. PROPERTIES OF THE POSITION OPERATOR WITH A GIVEN SPIN IN THE IRMM

According to the constraints imposed by symmetry presented in Section III, it is convenient to choose $m_\sigma = 1$

in Eq. (14) and its equivalent for spin down. The ISSHM (case $\Delta = 0$ of the IRMM) has inversion centers at the midpoint between two atomic positions, displaced a quarter of a unit cell from the atomic positions. Choosing the origin of coordinates at an atomic position, this implies that the inversion centers are located at $x_b = a/4$ plus a multiple of $a/2$. Using the filling conditions assumed $N_\uparrow = N_\downarrow = N_{uc}$, and $L = N_{uc}a$, Eq. (20) leads to

$$\tilde{R}U(1,0)\tilde{R}^\dagger = -\bar{U}(1,0), \quad (23)$$

and the same for spin down. This implies that the expectation values of $U(1,0)$ and $U(0,1)$ are purely imaginary in the ISSHM. Therefore from Eq. (1) α_σ ($\alpha(1,0)$ and $\alpha(0,1)$) can only take the values $\pm\pi/2 \bmod 2\pi$. Performing a similar calculation for $U(1,1)$ and $U(1,-1)$ it is easy to see that α_c and α_s can only take the values 0 or $\pi \bmod 2\pi$.

As an example, for $N_{uc} = 2$, $U = 0$ and $\delta = -t$, the ground state is $|g\rangle = \Pi_\sigma(c_{0\sigma}^\dagger + c_{1\sigma}^\dagger)(c_{2\sigma}^\dagger + c_{3\sigma}^\dagger)|0\rangle$. Using $x_j = bj$, where $b = a/2$, a straightforward calculation gives $\langle g|U(1,0)|g\rangle = \langle g|U(0,1)|g\rangle = -i/2$, and then $\alpha(1,0) = \alpha(0,1) = -\pi/2 \bmod 2\pi$. Changing the sign of δ corresponds to a translation of half a lattice parameter and the α_σ change sign.

A simple argument, validated by the numerical results presented below, is that for any parameters of the ISSHM, the expectation values of the position operators for a given spin are the same as the corresponding ones in which one has one localized particle at the midpoint of each strong bond. For negative δ , this means that the position of the particles with given spin are at $x_i = (i + 1/4)a$, $i = 0$ to $N_{uc} - 1$. Then $\sum_i x_i/L = 1/4 + (N_{uc} - 1)/2$, and using Eq. (1)

$$\begin{aligned} \alpha(1,0) = \alpha(0,1) &= (-1)^{N_{uc}-1} \frac{\pi}{2} \text{ if } \delta < 0, \\ \alpha(1,0) = \alpha(0,1) &= (-1)^{N_{uc}} \frac{\pi}{2} \text{ if } \delta > 0, \end{aligned} \quad (24)$$

where the last line was obtained from a translation of half a lattice parameter. Eqs. (24) are confirmed by the numerical calculations.

While for $\Delta = 0$, the system described by H has inversion symmetry at each lattice site [implying Eq. (19)] and for $\delta = 0$, the inversion points lie in between sites [implying Eq. (23)], at the special point $\Delta = \delta = 0$ both symmetry operations are present, and these equations imply that the expectation values of $U(1,0)$ and $U(0,1)$ should vanish. This fact suggests that the phases jump at this point. Numerically we find that $\alpha(1,0) = \alpha(0,1)$ jumps between $-\pi/2$ and $\pi/2$ for fixed $\Delta = 0$ changing δ and between 0 and π for fixed $\delta = 0$ changing Δ . The first jump is consistent with the two different topological sectors of the ISSHM¹³ and spin models related with it⁷⁷ as discussed in Section VIB.

For $U = 0$, and very small t , the second jump is expected from the phases for the states with occupancies

2020... and 0202... at both sides of the transition. Symmetry protection allows to extend the argument to large t . However, the physical meaning of the jump in the interacting case $U \neq 0$ (for which the system is in the MI phase of the IHM) is not clear.

VI. NUMERICAL RESULTS

In this Section we present results for the ground-state expectation value of the different position operators by exact diagonalization in systems between 6 and 14 sites, using the Lanczos method⁷⁵. We analyze the transitions of the corresponding topological Z_2 invariants in the IHM and ISSHM and its size dependence and compare them with alternative methods. This information is complemented studying pumping cycles in the general IRMM, including a staggered field and Ising spin-spin interactions.

A. Topological invariants in the IHM

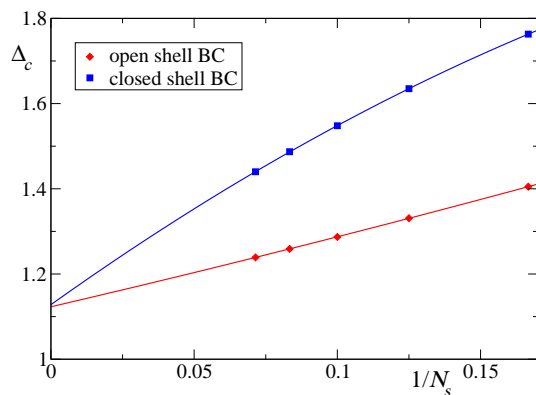


FIG. 1. (Color online) Critical value of Δ for the charge transition of the IHM as a function of the inverse of the number of sites for different boundary conditions. Other parameters are $t = 1$, $\delta = 0$ and $U = 4$. Full lines correspond to a parabolic fit.

As briefly explained in Section I, the phase diagram of the IHM has been determined by the MCEL which coincides with a jump in γ_c (γ_s) for the charge (spin) transition between BI and SDI (SDI and MI) phases (see Section IV for the explanation of the phases). Specifically the charge transition is determined by a crossing between the singlet state of lowest energy with even parity under inversion (the ground state in the BI phase) and the corresponding one for odd parity (the ground state in the SDI and MI phases) with OSBC [see Section II for a discussion on the boundary conditions (BC)]. In the spin transition between SDI and MI phases, for OSBC the excited even singlet crosses with the excited odd triplet, which has less energy in the MI phase^{36,66}.

To what extent do the topological invariants based on position operators reproduce these results?

The different $\alpha(m_\uparrow, m_\downarrow)$ are protected by inversion symmetry with center at each site and can take the values 0 or $\pi \bmod 2\pi$ (see Section III). We find that α_σ [see Eq. (14)] do not change at the transitions and has the value 0 (π) if the number of unit cells $N_{uc} = N_s/2$ is even (odd). We discuss this result in Section VI C. Instead, extrapolating the results of the jumps in α_c and α_s for adequate BC provide rather precise results.

In Fig. 1 we display the results for the jump in α_c at the charge transition for different system sizes and BC. We find that for most system sizes and OSBC, the value of Δ at the jump Δ_c coincides with the above mentioned crossing of levels. For 14 sites, α_c predicts a larger Δ_c (by about 0.003), but the difference is smaller than the size of the symbols in the figure. The results for CSBC have a larger size dependence, but the extrapolation to the thermodynamic limit using a parabola in $1/N_s$ for both sets of BC are very near each other ($\Delta_c = 1.123$ for OSBC, $\Delta_c = 1.128$ for CSBC). The parabola seems to fit well the data. In contrast, $\langle U(l, l) \rangle$ is expected to have a power-law dependence with a model-dependent exponent⁷⁶.

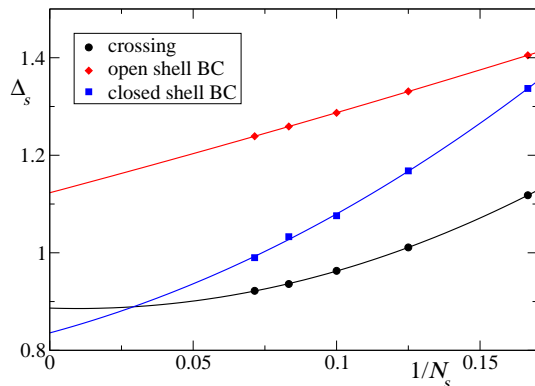


FIG. 2. (Color online) Critical value of Δ for the spin transition of the IHM as a function of the inverse of the number of sites for different boundary conditions, and compared with the crossing of excited levels. Other parameters are $t = 1$, $\delta = 0$ and $U = 4$. Full lines correspond to a parabolic fit.

In Fig. 2 we show the results of the spin transition and the more reliable result using the MCEL. A problem with the OSBC is that for $N_s \leq 12$ both α_c and α_s change abruptly with the ground state crossing with change of parity, and both Δ_c and Δ_s coincide. For 14 sites Δ_s is smaller as expected, but the difference is very small. Larger system sizes would be needed to correct this result. For the spin transition, the CSBC are more reliable, predicting an extrapolated value $\Delta_s = 0.836$ compared to $\Delta_s = 0.887$ of the MCEL.

B. Topological transitions in the ISSHM including J_z

Here we consider the Hamiltonian $H + H_z$, where the two terms are given in Eqs. (21) and (22), with $\Delta = 0$. The motivation is that for large U , this Hamiltonian reduces to an XXZ Heisenberg model with alternating bond interactions⁶⁶ similar to that studied by Tzeng *et al.*⁷⁷. This model has three phases, a Néel phase for small $|\delta|$ and two topologically different dimerized phases for large negative or positive δ .

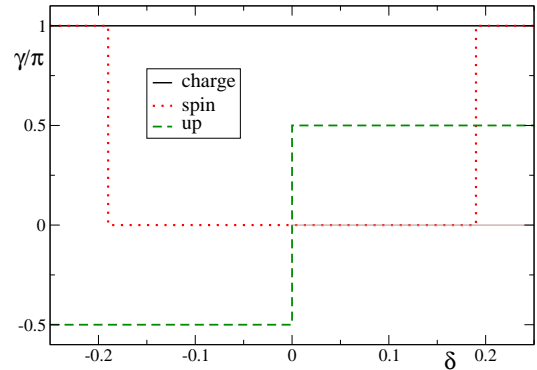


FIG. 3. (Color online) Topological invariants α_i as a function of the alternation in the hopping δ for $t = 1$, $\Delta = 0$, $U = 4$, $J_z = 0.4$ and 8 sites with OSBC. The result for spin down is the same as for spin up.

From the results of Section V one knows that the different α_i are topological invariants protected by inversion symmetry with center at the midpoint between any two sites. In Fig. 3 we show the different invariants as a function of δ . For $\delta = 0$, the system is in the MI phase of the IHM. As no charge transition takes place, α_c retains the same value π for finite δ . Instead, α_s shows jumps consistent with a transition from a Néel state at small $|\delta|$ to dimerized BOW phases at large $|\delta|$. In contrast, α_σ does not capture this transition, but it is able to differentiate between both BOW phases.

These results can be understood in simple terms. It is easy to check that for a state with all particles localized either in a Néel state ($\uparrow \downarrow \uparrow \downarrow \dots$) or an anti-Néel one ($\downarrow \uparrow \downarrow \uparrow \dots$), Eq. (1) gives $\alpha_s = \alpha(1, -1) = \pi \bmod 2\pi$. In a finite system, the ground state contains a mixture of both states and then, the position of the electrons with only one spin does not capture the antiferromagnetic correlation. Instead, both BOW phases can be distinguished by the value $\pm\pi/2 \bmod 2\pi$ of α_σ , as explained in Section V. However, for both BOW phases α_c (α_s) which represents the sum (difference) of the positions for both spins gives a result π (0) $\bmod 2\pi$.

Therefore, $\alpha_\uparrow = \alpha_\downarrow$ and α_s give complementary information and both are necessary and sufficient to characterize the different phases of the model.

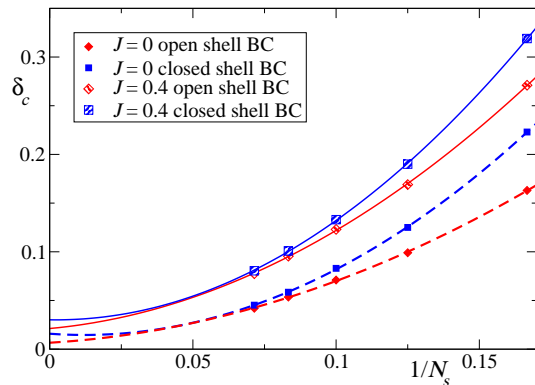


FIG. 4. (Color online) Critical value of δ for the Néel-BOW transition as a function of the inverse of the number of sites, for two values of J_z and different boundary conditions. Other parameters are $t = 1$, $\Delta = 0$, and $U = 4$.

In Fig. 4 we analyze the dependence on size and boundary conditions, for the transition between the Néel and BOW phases determined from the jump in α_s . The finite-size effects are rather large. For $J_z = 0$ and large U , the model is equivalent to a spin SU(2) invariant Heisenberg model with alternating bond interactions⁶⁶, and from results on the latter model^{78,79} one knows that a spin gap proportional to $|\delta|^{2/3}$ opens for small δ . Since the opening of a spin gap indicates a crossing of excited levels and a jump in the spin Berry phase to zero³³, one expects that in the thermodynamic limit, the value of δ at the transition $\delta_c \rightarrow 0$. If one estimates the error in δ_c from the difference between the extrapolated results for open- and closed-shell BC, the result for $J_z = 0$ is consistent with the expected result $\delta_c = 0$. Instead, for $J_z = 0.4$ the extrapolated results for δ_c (0.021 for OSBC and 0.030 for CSBC) suggest a small positive extrapolated value. To obtain more precise values of δ_c for small J_z , larger system sizes are needed.

C. Pumping circuits

When both Δ and δ are different from zero, all inversion symmetries are lost and most position expectation values lose their topological protection, except the spin one $\alpha(1, -1)$, which in absence of a staggered magnetic field, is protected by spin rotation symmetry of π around an axis perpendicular to the z one. To get further insight into the position expectation values and their related topological Z_2 invariants we have studied two pumping cycles of the form

$$\begin{aligned}\Delta &= \Delta_0 - 0.5t \cos \theta, \\ \delta &= 0.5t \sin \theta,\end{aligned}\quad (25)$$

where θ changes from 0 to 2π , in the IRMM with $N_\uparrow = N_\downarrow = N_{uc} = N_s/2$. The corresponding amount of elec-

trons transported in the cycle is expected to be

$$\Delta N_i = \frac{1}{2\pi} \int_0^{2\pi} d\theta \partial_\theta \alpha_i(\theta). \quad (26)$$

Multiplying this by the electronic charge $-e$, one has the corresponding charge transport [see Eqs. (12) and (13)]. We discuss below some subtleties related with ΔN_σ in the analysis of the numerical results.

We take $t = 1$ as the unit of energy, OSBC and $N_s = 8$. The results are very similar for other system sizes except for some details pointed out below.

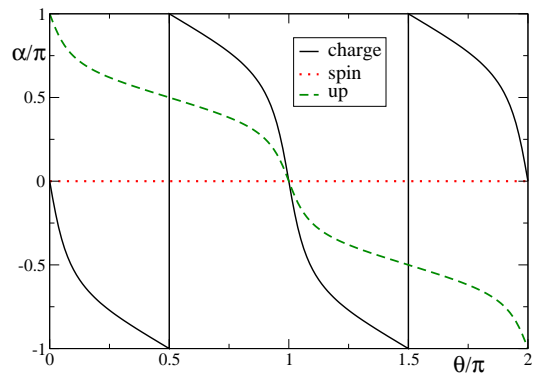


FIG. 5. (Color online) Indicators of the position of the particles in the pump cycle Eq. (25) for $N_s = 8$, OSBC, $t = 1$, $\Delta_0 = 0$, and $U = 1$.

For the first cycle, illustrated in Fig. 5, we take $\Delta_0 = 0$, and $U = 1$. For the chosen parameters and $\delta = 0$, the critical values of Δ for the charge and spin transition of the IHM lie at $\Delta_c = \Delta_s = \pm 0.177$. Then for $\theta = 0$ and $\theta = \pi$ the system is in the BI phase of the IHM, with site occupancies near 2020... in the first case and 0202... in the second one. As θ changes in the interval $0 < \theta < \pi$, with positive δ , the hopping between sites 0 and 1, 2 and 3, etc. is smaller in magnitude than that between 1 and 2, 3 and 4, etc. Therefore, as Δ changes from negative to positive values, the charges at the even sites displace towards the odd sites moving to the left, taking advantage of the larger magnitude of the hopping. In the remaining part of the cycle, δ changes sign and the particles continue displacing to the left from the odd sites to the even ones, to reach positions equivalent to the original one. This physical picture explains the results displayed in Fig. 5.

The results for spin up and down are the same. The physics is essentially the same as in the non-interacting RMM and for each spin, an electron is transported around the cycle. Note that for $\theta = 0$ and $\theta = \pi$, $\alpha_c = \alpha_s = 0$ as expected in the BI phase of the IHM. Also $\alpha_s = 0$ for all θ due to the presence of a spin gap. For $\theta = \pi/2$ ($3\pi/2$), Δ vanishes, the system is described by the ISSHM model with symmetry protected α_i , and

$\alpha_{\uparrow} = \alpha_{\downarrow} = \pi/2$ ($-\pi/2$) in agreement with Eqs. (24). For an even number of sites not multiple of four (odd $N_{uc} = N_s/2$), α_{σ} have almost the same dependence on θ but are shifted in π , as expected from Eqs. (24).

Note that in the whole cycle $\alpha_c = \alpha_{\uparrow} + \alpha_{\downarrow}$, and $\alpha_s = \alpha_{\uparrow} - \alpha_{\downarrow}$, so that in this case, both α_{σ} contain the whole information. The same happens in the general case in the presence of a staggered field (shown below) which isolates the ground state from the remaining states breaking the degeneracies for all parameters⁶⁶.

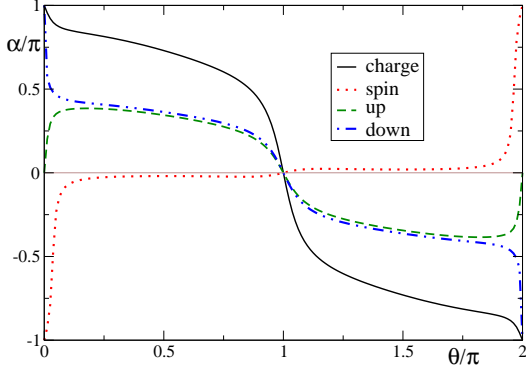


FIG. 6. (Color online) Same as Fig. 5 for $\Delta_0 = 1.3$, and $U = 4$ and including $B = 0.2$.

In the second cycle considered, corresponding to Fig. 6 we take $\Delta_0 = 1.3$, and $U = 4$. For $\delta = 0$, we obtain $\Delta_c = \Delta_s = \pm 1.739$. Then for $\theta = 0$ the system is in the MI phase of the IHM, while for $\theta = \pi$, the system is in the BI phase of the model. We have added first a staggered magnetic field H_B [see Eq. (22)], which simplifies the qualitative analysis in terms of quasi localized charges (that would correspond to small hopping amplitudes). For $\theta = 0$, the dominant configuration is $\downarrow\uparrow\downarrow\uparrow\ldots$ for sites $0,1,2,3 \ldots$ while for $\theta = \pi$ the dominant configuration is $0202\ldots$. Since in the interval $0 < \theta < \pi$, the hopping between sites 1 and 2, 3 and 4, etc is more favorable than the remaining ones, as θ increases, the electrons with spin down move to the left from the even to the odd sites. In the remaining part of the cycle $\pi < \theta < 2\pi$, also the electrons with spin down move from the doubly occupied odd sites to the left reproducing the original configuration.

The evolution of the different expectation values for this case is shown in Fig. 6. They are topologically protected by inversion symmetry at each site only for $\theta = 0$ and $\theta = \pi$, where they have the value either 0 or π . In agreement with the argument above, at the end of the cycle, an electron with spin down is pumped one unit cell to the left, while no net transport takes place for spin up. However, for small staggered field B , the difference between both spins is only important near the MI phase (small $\theta \bmod 2\pi$). For other values of θ , α_{σ} are qualitatively similar but of smaller magnitude, as the result

for the previous cycle. As before, for an even number of sites not multiple of four, α_{σ} are shifted in π . We note that if pure spin pumping without charge pumping is wished, one can change the cycle to that of the shape of an eight⁶⁶ or changing the staggered field in the limit of large U ⁸⁰. In this limit, the model is equivalent to a Heisenberg model with alternating Heisenberg interaction⁶⁶ with a staggered magnetic field, in which spin pumping is possible⁸⁰ and similar to the effective model that corresponds to an experimental implementation of a spin pump with ultracold bosonic atoms in an optical superlattice⁶².

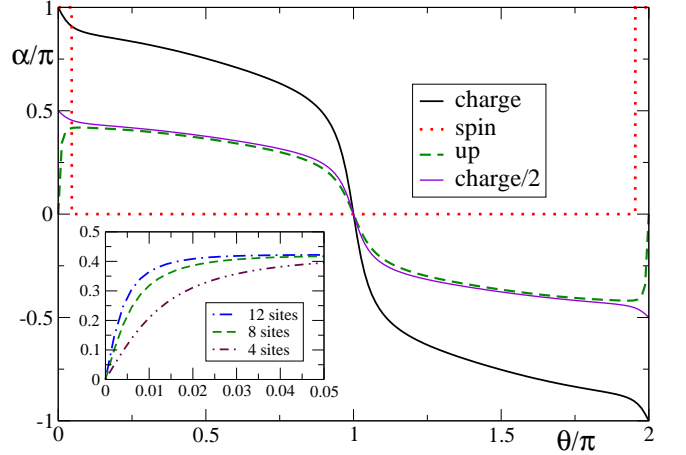


FIG. 7. (Color online) Same as Fig. 6 for $B = 0$. The inset shows α_{σ} for several system sizes.

In Fig. 7 we present the different position expectation values for the IRMM with $B = 0$, restoring spin $SU(2)$ symmetry. For $\delta = 0$, one has $\Delta_c = \Delta_s = \pm 1.331$ (as already displayed in Figs. 1 and 2), therefore, as in Fig. 6, the critical points lie inside the cycle given by Eq. (25). For both figures, the results for α_c and α_s are consistent with previous results, including time-dependent calculations of the charge transport⁶⁶ indicating that a total of one charge (and no spin in this case) is transported in the cycle. Instead, in this case with $B = 0$, the results for $\alpha_{\uparrow} = \alpha_{\downarrow}$ predict no charge transport in contradiction to the previous results. Note that α_{σ} is very near $\alpha_c/2$ except near the MI phase θ near $0 \bmod 2\pi$ for which important finite-size effects occur. In fact, as discussed in Section VIB for $\Delta = 0$, α_s is expected to be 0 for any $\theta \neq 0$ and the value π near $\theta = 0$ is also a finite-size effect⁶⁶.

The size dependence suggests that in the thermodynamic limit $\alpha_{\sigma} \rightarrow \alpha_c/2$ and half an electron with spin σ is transported in the cycle from $\theta = \epsilon$ to $\theta = 2\pi - \epsilon$ with $\epsilon \rightarrow 0$. For $L \rightarrow \infty$, as the system passes through the MI phase ($\theta = \delta = 0$), there is a transition between the two possible BOW phases⁶⁶ (or spin dimerized phases for large U ^{66,77}). The BOW order parameter is singular:

$$O_{\text{BOW}} = \frac{1}{L} \sum_j (-1)^j \langle c_{j+1\sigma}^\dagger c_{j\sigma} + \text{H.c.} \rangle \sim \delta^{1/3}. \quad (27)$$

This explains the discontinuity in α_σ in the thermodynamic limit. As a consequence, Eq. (26) for $i = \sigma$ which assumes a non-degenerate smooth ground state fails for $L \rightarrow \infty$ for a path that passes through $\theta = 0$. For a finite system, there is no singularity at $\theta = \delta = 0$, but the inversion symmetry imposes that α_σ should be either 0 or π leading to large finite-size effects, that are apparent in Fig. 7. Instead, α_c is continuous and well behaved near $\theta = 0$. Summarizing these results, one electron is transported in the cycle, in agreement with previous time-dependent calculations⁶⁶ and half of it corresponds to each spin.

We have also studied the effect of adding a Zeeman term H_Z [see Eq. (22)] to the results shown in Fig. 7. The results are qualitatively very similar and therefore are not shown. However, in this case, we expect that in the thermodynamic limit for small θ (implying small δ) there is a spontaneous symmetry breaking between the Néel and anti-Néel states, and the behavior of the α_σ would be similar to that shown in Fig. 6 but with $B \rightarrow 0$.

VII. SUMMARY AND DISCUSSION

We have studied the general properties of topological Z_2 invariants based on position operators of the form of Eqs. (1) and (2). For the expectation values to be well defined, m_σ should be integers, and in some cases different from ± 1 . In addition, Eq. (17) should be satisfied.

In general, $\alpha(m_\uparrow, m_\downarrow)$ gives the same information as the corresponding Berry phase, except for the sign and quantitative but not qualitative differences due to finite-size effects. In some cases, there is a shift between both quantities, but the changes in polarization coincide except for finite-size effects. For small systems, the jumps in Berry phases provide more accurate results for topological transitions, but the $\alpha(m_\uparrow, m_\downarrow)$ are easier to calculate,

and using different boundary conditions an accurate extrapolation to the thermodynamic limit can be obtained. In addition, open boundary conditions can be used⁷⁰ and the formalism can be extended to finite temperature¹⁴.

For the interacting Rice-Mele model, $\alpha_c = \alpha(1, 1)$, $\alpha_s = \alpha(1, -1)$, $\alpha_\uparrow = \alpha(1, 0)$ give complementary information and using all of them, one can determine the different topological sectors of the model and construct the different phase diagrams. For some parameters, the model reduces to the ionic Hubbard model (IHM) and for others to the interacting Su-Schrieffer-Heeger model (ISSHM). In both cases, the α_i are topological Z_2 numbers protected by different inversion symmetries. For the case of the IHM, α_c and α_s are enough to determine the phase transitions, while α_\uparrow does not show any jumps. The spin transition converges faster to the thermodynamic limit if closed shell boundary conditions (antiperiodic for a number of sites multiple N_s of 4, periodic for even N_s not multiple of 4) are used. For the ISSHM including Ising spin-spin interactions, the jumps in α_s (which can take the values 0 or $\pi \bmod 2\pi$) and α_\uparrow (which can take the values $\pm\pi/2 \bmod 2\pi$) identify the phase transitions, while α_c is featureless.

The pump cycles shown in Section VIC reveal subtle finite-size effects in α_σ near vanishing hopping alternation. They are related with closing gaps in the thermodynamic limit.

Our study was limited to $SU(2)$ symmetry in the spin sector and one dimension but it can be generalized to $SU(N)$ systems, like half-filled two-orbital ones⁸¹ and others¹⁶, and more dimensions. In addition, more information can be extracted using the cumulants of the topological indicators⁵¹⁻⁵⁵

ACKNOWLEDGMENTS

We thank E. Bertok and F. Heidrich-Meisner for useful discussions. We acknowledge financial support provided by PICT 2017-2726 and PICT 2018-01546 of the AN-PCyT, Argentina.

¹ L. D. Landau and E. Lifshitz, *Statistical Physics, (Course of Theoretical Physics, Volume 5)* (Butterworth-Heinemann, 1980).

² A. P. Schnyder, S. Ryu, A. Furusaki, and A. W. W. Ludwig, Classification of topological insulators and superconductors in three spatial dimensions Phys. Rev. B **78**, 195125 (2008).

³ A. Kitaev, Periodic table for topological insulators and superconductors, AIP Conf. Proc. **1134**, 22 (2009).

⁴ M. Z. Hasan and C. L. Kane, Topological Insulators, Rev. Mod. Phys. **82**, 3045 (2010).

⁵ R.-J. Slager, A. Mesaros, V. Jurić, and J. Zaanen The space group classification of topological band-insulators, Nat. Physics **9**, 98 (2013).

⁶ Y. Ando, Topological Insulator Materials, J. Phys. Soc. Jpn. **82**, 102001 (2013).

⁷ C.-K. Chiu, J. C. Y. Teo, A. P. Schnyder, and S. Ryu, Classification of topological quantum matter with symmetries, Rev. Mod. Phys. **88**, 035005 (2016).

⁸ B. Bradlyn, L. Elcoro, J. Cano, M. G. Vergniory, Z. Wang, C. Felser, M. I. Aroyo, and B. A. Bernevig, Topological quantum chemistry, Nature **547**, 298 (2017).

- ⁹ J. Kruthoff, Jan de Boer, J. van Wezel, C. L. Kane, and R.-J. Slager, Topological Classification of Crystalline Insulators through Band Structure Combinatorics, *Phys. Rev. X* **7**, 041069 (2017).
- ¹⁰ J. Wang and S.-C. Zhang Topological states of condensed matter, *Nature Mat.* **16**, 1062 (2017).
- ¹¹ A. Montorsi, F. Dolcini, R. C. Iotti, and F. Rossi, Symmetry-protected topological phases of one-dimensional interacting fermions with spin-charge separation, *Phys. Rev. B* **95**, 245108 (2017).
- ¹² V. Gurarie, Single-particle Green's functions and interacting topological insulators, *Phys. Rev. B* **83**, 085426 (2011).
- ¹³ S. R. Manmana, A. M. Essin, R. M. Noack, and V. Gurarie, Topological invariants and interacting one-dimensional fermionic systems, *Phys. Rev. B* **86**, 205119 (2012).
- ¹⁴ R. Unanyan, M. Kiefer-Emmanouilidis, and M. Fleischhauer, Finite-Temperature Topological Invariant for Interacting Systems, *Phys. Rev. Lett.* **125**, 215701 (2020).
- ¹⁵ A. Montorsi, U. Bhattacharya, Daniel González-Cuadra, M. Lewenstein, G. Palumbo, and L. Barbiero, Interacting second-order topological insulators in one-dimensional fermions with correlated hopping, arXiv:2208.00939
- ¹⁶ B. Ostahie, D. Sticlet, C. P. Moca, B. Dóra, M. A. Werner, J. K. Asbóth, and G. Zaránd, Multiparticle quantum walk in the strongly interacting SU(3) Su-Schrieffer-Heeger-Hubbard topological model, arXiv:2209.03569
- ¹⁷ R. Žitko, G. G. Blesio, L. O. Manuel and A. A. Aligia, Iron phthalocyanine on Au(111) is a “non-Landau” Fermi liquid, *Nature Commun.* **12**, 6027 (2021).
- ¹⁸ J. Zak, Berry's phase for energy bands in solids, *Phys. Rev. Lett.* **62**, 2747 (1989).
- ¹⁹ S. Tewari and J. D. Sau, Topological Invariants for Spin-Orbit Coupled Superconductor Nanowires, *Phys. Rev. Lett.* **109**, 150408 (2012).
- ²⁰ J.K. Asbóth, L. Oroszlány, and A. Pályi, **A short course on topological insulators**, Lecture Notes in Physics, 2016. ISSN 1616-6361. doi: 10.1007/978-3-319-25607-8.
- ²¹ F. Cardano, A. D'Errico, A. Dauphin, M. Maffei, B. Piccirillo, C. de Lisio, G. De Filippis, V. Cataudella, E. Santamato, L. Marrucci, M. Lewenstein, and P. Massignan, Detection of Zak phases and topological invariants in a chiral quantum walk of twisted photons, *Nat. Commun.* **8**, 15516 (2017).
- ²² D. Pérez Daroca and A. A. Aligia Phase diagram of a model for topological superconducting wires, *Phys. Rev. B* **104**, 115125 (2021).
- ²³ R. Resta, Macroscopic polarization in crystalline dielectrics: the geometric phase approach. *Rev. Mod. Phys.* **66**, 899 (1994).
- ²⁴ D. Xiao, M.-C. Chang, and Q. Niu, Berry phase effects on electronic properties, *Rev. Mod. Phys.* **82**, 1959 (2010).
- ²⁵ D. Vanderbilt, *Berry Phases in Electronic Structure Theory: Electric Polarization, Orbital Magnetization and Topological Insulators*, (Cambridge University Press, 2018).
- ²⁶ B. Bradlyn, and M. Iraola, Lecture notes on Berry phases and topology, *SciPost Phys. Lect. Notes* 51 (2022).
- ²⁷ G. Ortiz and R. M. Martin, Macroscopic polarization as a geometric quantum phase: Many-body formulation, *Phys. Rev. B* **49**, 14202 (1994).
- ²⁸ R. Resta and S. Sorella, Many-Body Effects on Polarization and Dynamical Charges in a Partly Covalent Polar Insulator, *Phys. Rev. Lett.* **74**, 4738 (1995).
- ²⁹ G. Ortiz, P. Ordejón, R. M. Martin, and G. Chiappe, Quantum phase transitions involving a change in polarization, *Phys. Rev. B* **54**, 13515 (1996).
- ³⁰ X.-Y. Song, Y.-C. He, A. Vishwanath, and C. Wang, Electric polarization as a nonquantized topological response and boundary Luttinger theorem, *Phys. Rev. Research* **3**, 023011 (2021).
- ³¹ W. A. Wheeler, L. K. Wagner, and T. L. Hughes Many-body electric multipole operators in extended systems, *Phys. Rev. B* **100**, 245135 (2019).
- ³² M. Tahir and H. Chen, Current-induced quasiparticle magnetic multipole moments, arXiv:2210.15753.
- ³³ A. A. Aligia, Berry phases in superconducting transitions, *Europhys. Lett.* **45**, 411 (1999).
- ³⁴ A. A. Aligia, K. Hallberg, C.D. Batista and G. Ortiz, Phase diagrams from topological transitions: The Hubbard chain with correlated hopping, *Phys. Rev. B* **61**, 7883 (2000).
- ³⁵ M.E. Torio, A.A. Aligia, K. Hallberg and H.A. Ceccatto, Phase diagram of the extended Hubbard chain with charge-dipole interactions, *Phys. Rev. B* **62**, 6991 (2000)
- ³⁶ M. E. Torio, A. A. Aligia, and H. A. Ceccatto, Phase diagram of the Hubbard chain with two atoms per cell, *Phys. Rev. B* **64**, 121105(R) (2001).
- ³⁷ M. E. Torio, A. A. Aligia, and H. A. Ceccatto, Phase diagram of the $t - t' - U$ chain at half filling, *Phys. Rev. B* **67**, 165102 (2003) (6 pages)
- ³⁸ K. Nomura and K. Okamoto, Critical properties of $S = 1/2$ antiferromagnetic XXZ chain with next-nearest-neighbour interactions, *J. Phys. A* **27**, 5773 (1994).
- ³⁹ M. Nakamura, K. Nomura, and A. Kitazawa, Renormalization Group Analysis of the Spin-Gap Phase in the One-Dimensional $t - J$ Model, *Phys. Rev. Lett.* **79**, 3214 (1997).
- ⁴⁰ M. Nakamura, Mechanism of CDW-SDW Transition in One Dimension, *J. Phys. Soc. Jpn.* **68**, 3123 (1999).
- ⁴¹ M. Nakamura, Tricritical behavior in the extended Hubbard chains, *Phys. Rev. B* **61**, 16377 (2000).
- ⁴² R. D. Somma and A. A. Aligia, Phase diagram of the XXZ chain with next-nearest-neighbor interactions, *Phys. Rev. B* **64**, 024410 (2001).
- ⁴³ G. I. Japaridze and A. P. Kampf, Weak-coupling phase diagram of the extended Hubbard model with correlated-hopping interaction, *Phys. Rev. B* **59**, 12822 (1999).
- ⁴⁴ A. A. Aligia and L. Arrachea, Triplet superconductivity in quasi-one-dimensional systems *Phys. Rev. B* **60**, 15332 (1999).
- ⁴⁵ R. Resta, Quantum-Mechanical Position Operator in Extended Systems, *Phys. Rev. Lett.* **80**, 1800 (1998).
- ⁴⁶ R. Resta and S. Sorella, Electron Localization in the Insulating State, *Phys. Rev. Lett.* **82**, 370 (1999).
- ⁴⁷ A. A. Aligia and G. Ortiz, Quantum Mechanical Position Operator and Localization in Extended Systems, *Phys. Rev. Lett.* **82**, 2560 (1999).
- ⁴⁸ G. Ortiz and A. A. Aligia, How localized is an extended quantum system ?, *Phys. Status Solidi B* **220**, 737 (2000).
- ⁴⁹ M. Nakamura and S. Todo, Order Parameter to Characterize Valence-Bond-Solid States in Quantum Spin Chains *Phys. Rev. Lett.* **89**, 077204 (2002).
- ⁵⁰ C. D. Batista, G. Ortiz, and A. A. Aligia, Ferrotoroidic Moment as a Quantum Geometric Phase, *Phys. Rev. Lett.* **101**, 077203 (2008).
- ⁵¹ I. Souza, T. Wilkens, and R. M. Martin, Polarization and localization in insulators: Generating function approach, *Phys. Rev. B* **62**, 1666 (2000).

- ⁵² G. Ortiz and A. A. Aligia, How Localized is an Extended Quantum System? *Physica Status Solidi (b)* **220**, 737 (2000).
- ⁵³ B. Hetényi and B. Dóra, Quantum phase transitions from analysis of the polarization amplitude, *Phys. Rev. B* **99**, 085126 (2019).
- ⁵⁴ B. Hetényi, Interaction-driven polarization shift in the $t - V - V'$ lattice fermion model at half filling: Emergent Haldane phase, *Phys. Rev. Research* **2**, 023277 (2020).
- ⁵⁵ B. Hetényi and S. Cengiz, Geometric cumulants associated with adiabatic cycles crossing degeneracy points: Application to finite size scaling of metal-insulator transitions in crystalline electronic systems, *Phys. Rev. B* **106**, 195151 (2022).
- ⁵⁶ B. Hetényi, S. Parlak, and M. Yahyavi, Scaling and renormalization in the modern theory of polarization: Application to disordered systems, *Phys. Rev. B* **104**, 214207 (2021).
- ⁵⁷ D. J. Thouless, Quantization of particle transport, *Phys. Rev. B* **27**, 6083 (1983).
- ⁵⁸ Q. Niu and D. J. Thouless, Quantised adiabatic charge transport in the presence of substrate disorder and many-body interaction, *J. Phys. A: Math. Gen.* **17**, 2453 (1984).
- ⁵⁹ S. Nakajima, T. Tomita, S. Taie, T. Ichinose, H. Ozawa, L. Wang, M. Troyer, and Y. Takahashi, Topological Thouless pumping of ultracold fermions, *Nat. Phys.* **12**, 296 (2016).
- ⁶⁰ M. Lohse, C. Schweizer, O. Zilberberg, M. Aidelsburger, and I. Bloch, A Thouless quantum pump with ultracold bosonic atoms in an optical superlattice *Nat. Phys.* **12**, 350 (2016).
- ⁶¹ M. J. Rice and E. J. Mele, Elementary Excitations of a Linearly Conjugated Diatomic Polymer, *Phys. Rev. Lett.* **49**, 1455 (1982).
- ⁶² C. Schweizer, M. Lohse, R. Citro, and I. Bloch, Spin Pumping and Measurement of Spin Currents in Optical Superlattices, *Phys. Rev. Lett.* **117**, 170405 (2016).
- ⁶³ A.-S. Walter, Z. Zhu, M. Gächter, J. Minguzzi, S. Roschinski, K. Sandholzer, K. Viebahn, and T. Esslinger, Breakdown of quantisation in a Hubbard-Thouless pump *arXiv:2204.06561*.
- ⁶⁴ M. Nakagawa, T. Yoshida, R. Peters, and N. Kawakami, Breakdown of topological Thouless pumping in the strongly interacting regime, *Phys. Rev. B* **98**, 115147 (2018).
- ⁶⁵ L. Stenzel, A. L. C. Hayward, C. Hubig, U. Schollwöck, and F. Heidrich-Meisner, Quantum phases and topological properties of interacting fermions in one-dimensional superlattices, *Phys. Rev. A* **99**, 053614 (2019).
- ⁶⁶ E. Bertok, F. Heidrich-Meisner, and A. A. Aligia, Splitting of topological charge pumping in an interacting two-component fermionic Rice-Mele Hubbard model, *Phys. Rev. B* **106**, 045141 (2022).
- ⁶⁷ R. Citro and M. Aidelsburger, Thouless pumping and topology, *arXiv:2210.02050*, *Nature Reviews Physics* (2023) DOI: 10.1038/s42254-022-00545-0.
- ⁶⁸ W. P. Su, J. R. Schrieffer, and A. J. Heeger, Solitons in Polyacetylene, *Phys. Rev. Lett.* **42**, 1698 (1979).
- ⁶⁹ P. Mognini and N. Cooper, Topological phase transitions at finite temperature, *arXiv:2208.08994*
- ⁷⁰ R. Li and M. Fleischhauer, Finite-size corrections to quantized particle transport in topological charge pumps, *Phys. Rev. B* **96**, 085444 (2017).
- ⁷¹ M. Fabrizio, A.O. Gogolin, and A.A. Nersisyan, From Band Insulator to Mott Insulator in One Dimension, *Phys. Rev. Lett.* **83**, 2014 (1999).
- ⁷² S. R. Manmana, V. Meden, R. M. Noack, and K. Schönhammer, Quantum critical behavior of the one-dimensional ionic Hubbard model, *Phys. Rev. B* **70**, 155115 (2004).
- ⁷³ M. E. Torio, A. A. Aligia, G. I. Japaridze, and B. Normand, Quantum phase diagram of the generalized ionic Hubbard model for AB_n chains, *Phys. Rev. B* **73**, 115109 (2006).
- ⁷⁴ A. A. Aligia, Charge dynamics in the Mott insulating phase of the ionic Hubbard model, *Phys. Rev. B* **69**, 041101(R) (2004).
- ⁷⁵ C. Lanczos, An iteration method for the solution of the eigenvalue problem of linear differential and integral operators, *J. Res. Nat. Bur. Std.* **45**, 225 (1950).
- ⁷⁶ R. Kobayashi, Y. O. Nakagawa, Y. Fukusumi, and M. Oshikawa, Scaling of the polarization amplitude in quantum many-body systems in one dimension *Phys. Rev. B* **97**, 165133 (2018).
- ⁷⁷ Y.-C. Tzeng, L. Dai, M.-C. Chung, L. Amico, and L.-C. Kwek, Entanglement convertibility by sweeping through the quantum phases of the alternating bonds XXZ chain, *Sci. Rep.* **6**, 26453 (2016).
- ⁷⁸ M. C. Cross and D. S. Fisher, A new theory of the spin-Peierls transition with special relevance to the experiments on TTFCuBDT, *Phys. Rev. B* **19**, 402 (1979).
- ⁷⁹ K. Okamoto, H. Nishimori, and Y. Taguchi, A numerical study of spin-1/2 alternating antiferromagnetic Heisenberg linear chains, *J. Phys. Soc. Jpn.* **55**, 1458 (1986).
- ⁸⁰ R. Shindou, Quantum Spin Pump in $S=1/2$ Antiferromagnetic Chains – Holonomy of Phase Operators in sine-Gordon Theory, *J. Phys. Soc. Jpn.* **74**, 1214 (2005).
- ⁸¹ V. Bois, S. Capponi, P. Lecheminant, M. Moliner, and K. Totsuka, *Phys. Rev. B* **91**, 075121 (2015).